CLASSE
Cornell Laboratory for Accelerator-based ScienceS & Education

The Center for BRIGHT BEAMS
A National Science Foundation Science & Technology Center

Brookhaven National Laboratory

U.S. DEPARTMENT OF ENERGY

Machine Learning Applications for Improving Accelerator Operations at the AGS and AGS Booster

Lucy Lin

Advisor: Georg Hoffstaetter de Torquat

CBB BDC Theme Meeting

August 31, 2023

@BrookhavenLab

Summary

- Machine learning for better orbit correction at the Alternating Gradient Synchrotron

- Generalized Gradient Map Tracking in the Siberian Snakes of the Alternating Gradient Synchrotron

- Current to magnet strength calibration with neural network at the Alternating Gradient Synchrotron Booster

Motivation: EIC cooler, higher polarization

- Booster and the AGS serve as injectors to RHIC and future EIC, which require small incoming emittance for electron cooling
- EIC requires pre-cooler at RHIC injection energy (AGS extraction energy)
- Currently Booster and AGS lack systematic tuning routine, mostly hand tuned by operators
- Algorithm to better control beam in the injector compound will be helpful to produce brighter beam with higher polarization in RHIC and EIC

Injector compound for RHIC and EIC

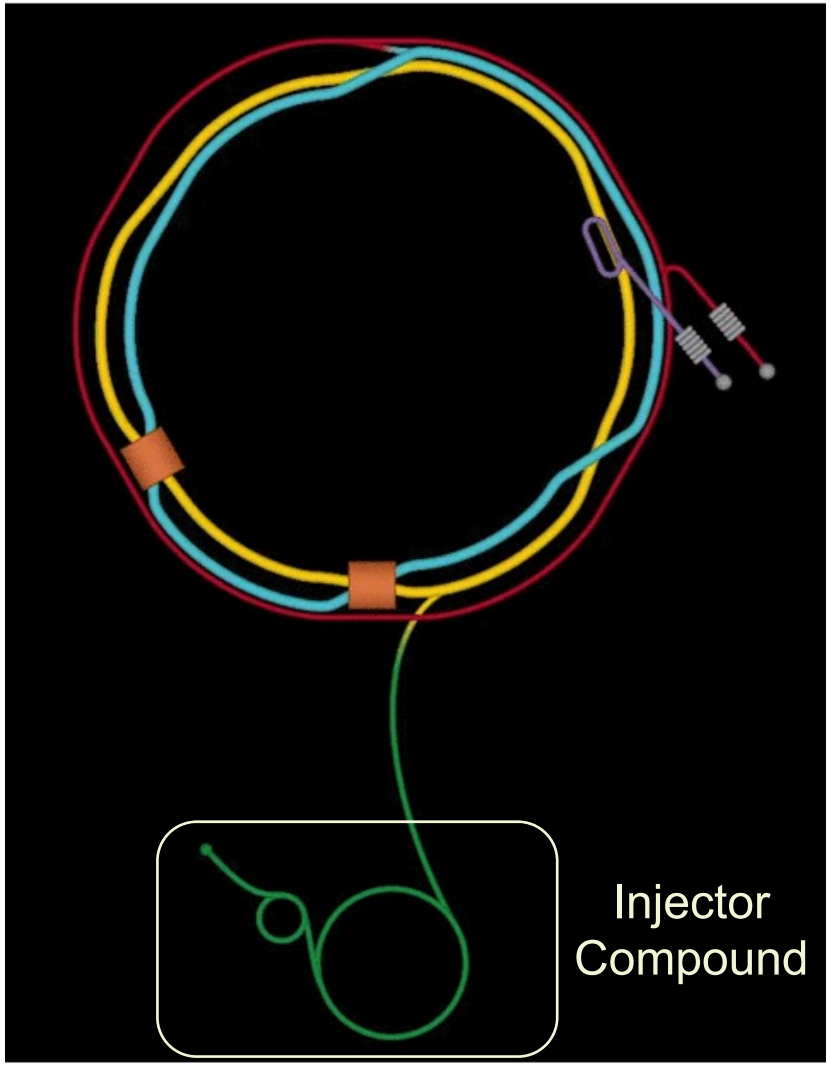

- **Relativistic Heavy Ion Collider (RHIC)**: largest operating accelerator in the US.
- **Electron Ion Collider (EIC)**: the nation's largest particle accelerator project.
- **Alternating Gradient Synchrotron** (AGS) and its **Booster** serve as part of the **injector compound** for RHIC and future EIC.
- **Bright ion beams** in the AGS and Booster are required for optimal luminosity and highest polarization in RHIC and EIC.
- Obtaining bright beam requires **more accurate beam control** in the injector compound, which is currently mostly hand tuned by operators.

Machine Learning for Better Orbit Correction at the Alternating Gradient Synchrotron

Brookhaven National Laboratory

CLASSE
Cornell Laboratory for Accelerator-based ScienceS & Education

Alternating Gradient Synchrotron (AGS)

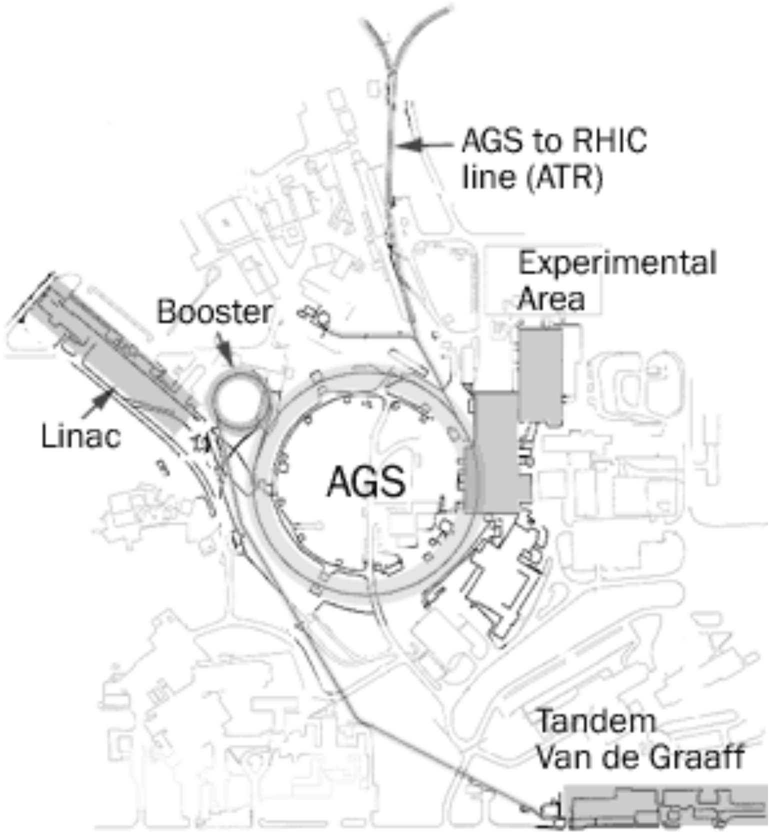

- Alternating gradient / strong focusing principle: achieve strong vertical and horizontal focusing of charged particle beam at the same time
- Accelerates proton to 33 GeV in 1960
- 12 super-periods (A to L), 240 main magnets, 810 m circumference
- Now serves as injector for Relativistic Heavy Ion Collider (RHIC)

Brookhaven National Laboratory
CLASSE Cornell Laboratory for Accelerator-based ScienceS & Education

Orbit Response at the AGS

- 72 pick-up electrodes (PUE), 48 horizontal and vertical corrector pairs
- Traditional orbit correction
  - obtain mapping from corrector settings $\vec{\theta}$ to orbit measurements $\vec{y}$
  - inverse mapping to get corrector settings $\Delta\vec{\theta}$ needed to cancel orbit deviations $\Delta\vec{y}$

$$\begin{pmatrix} \Delta\vec{x} \\ \Delta\vec{y} \end{pmatrix} = \underline{R} \begin{pmatrix} \Delta\vec{\theta}_x \\ \Delta\vec{\theta}_y \end{pmatrix}$$

$$\frac{\Delta x_i}{\Delta\theta_j} = R_{ij}$$

Orbit Correction with Neural Network

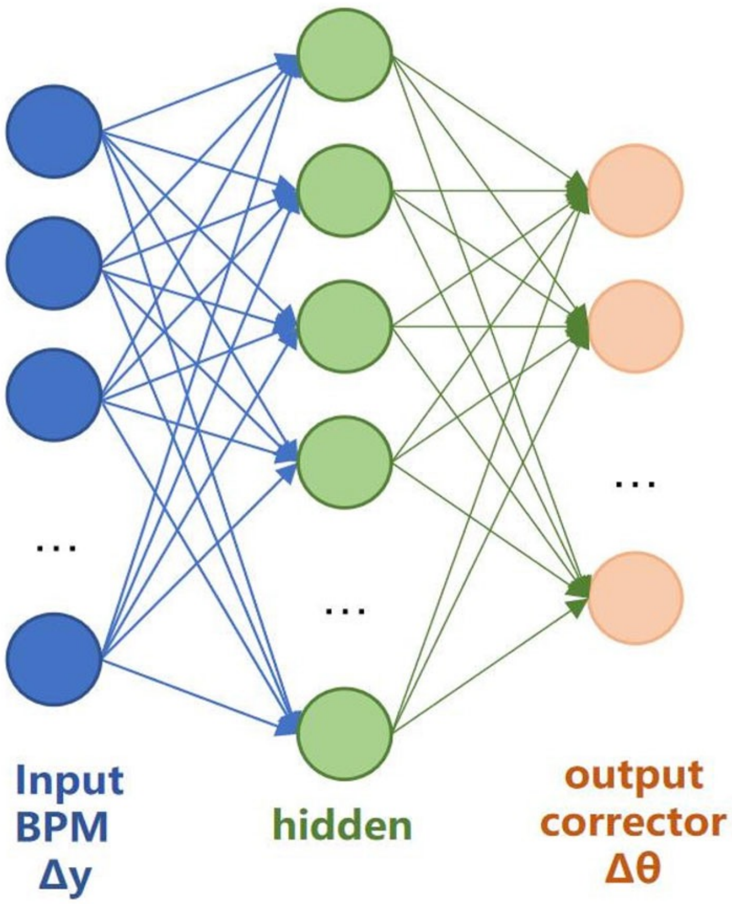

- Need dedicated machine time to measure a full orbit response matrix: at least 30 min
- Pre-measured mapping gets less accurate with time → orbit drift / brightness drop
- Orbit correction with NN
  - train directly to get inverse mapping, no need for extra calculation
  - easily update with new data and stay accurate

ML method: Neural Network (NN)

- Establish mapping between a given set of inputs $\vec{X}$ and corresponding outputs $\vec{Y}$
- Fully connected layers: output = activation(dot(input, weight) + bias)
- Activation function: Hyperbolic Tangent (Tanh) and Rectified Linear Unit (ReLU)
- Feed forward neural network (FFNN): most common, no feedback route

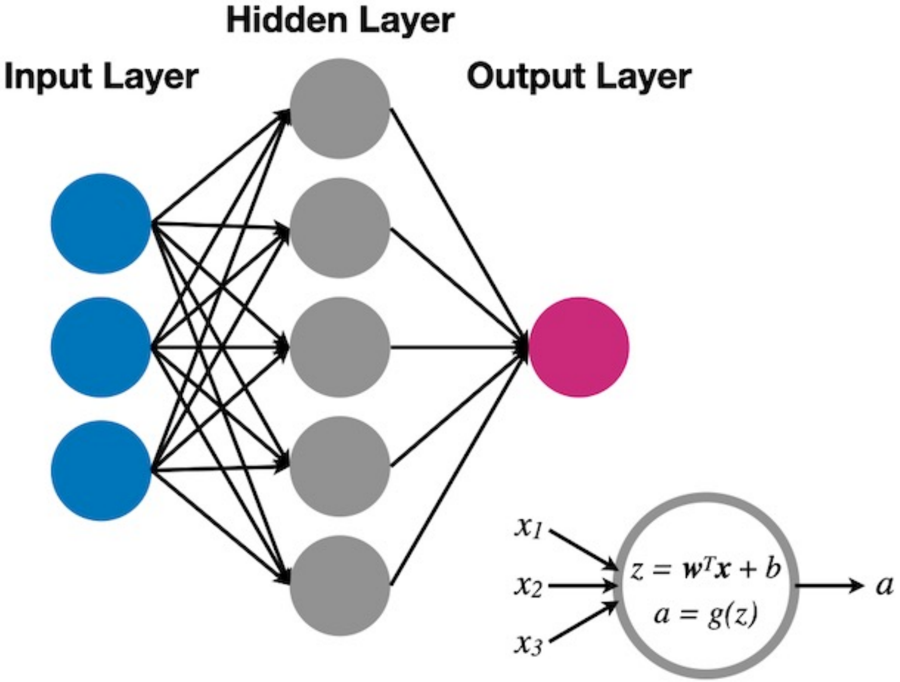

Hyperbolic tangent	$\phi(z) = \dfrac{e^z - e^{-z}}{e^z + e^{-z}}$	Multi-layer Neural Networks	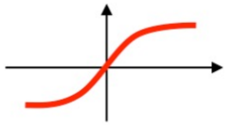
Rectifier, ReLU (Rectified Linear Unit)	$\phi(z) = max(0, z)$	Multi-layer Neural Networks	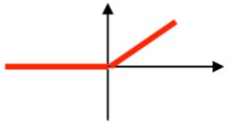

ORM NN model: training results

- Input 48 vertical corrector kick → Output 72 y orbit measured at BPM
- Trained on 800 data pairs, tested on 200 data pairs: R^2 score = 0.998

$$R^2 = 1 - \frac{\sum(y_i - \hat{y}_i)^2}{\sum(y_i - \overline{y}_i)^2}$$

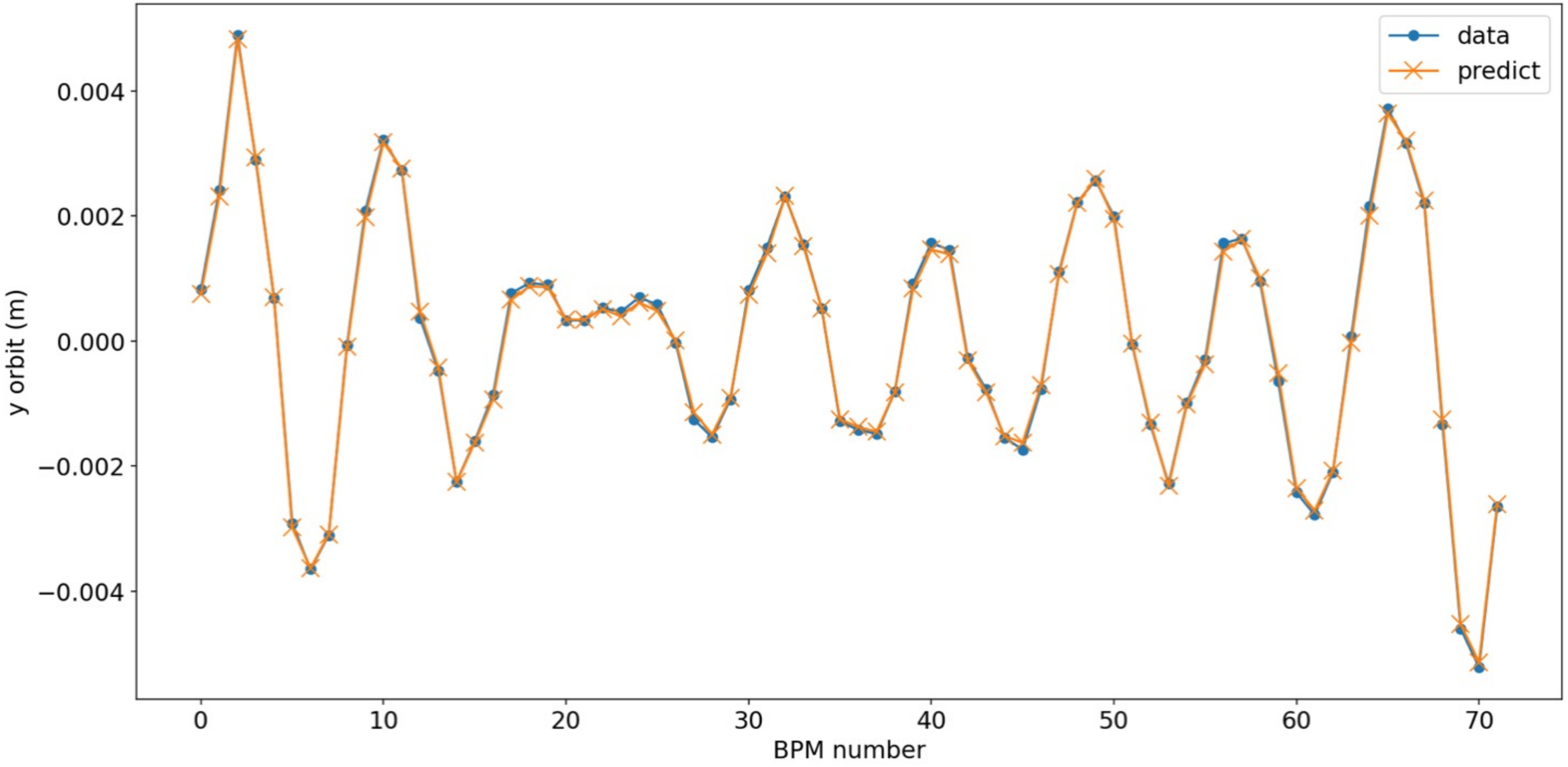

Inverse ORM NN model: training results

- Input 72 y orbit measured at BPM → Output 48 vertical corrector kick
- Trained on 800 data pairs, tested on 200 data pairs: R^2 score = 0.993

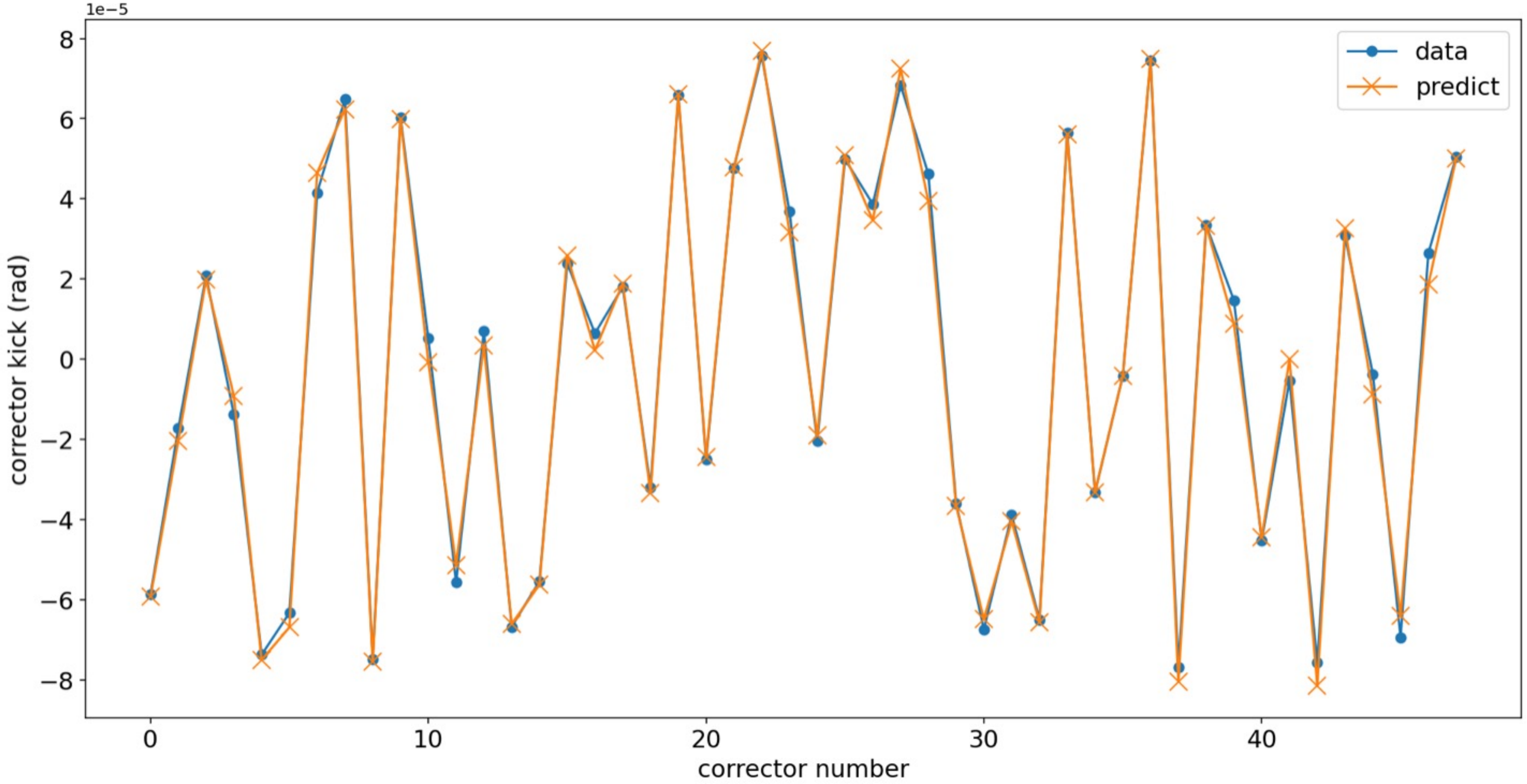

Future work: error identification

- Neural network can establish mapping between any inputs and outputs with sufficient data
- Machine error sources (e.g., misalignment, gradient / calibration errors, etc.) can be included as outputs of an inverse NN model for beam-based error diagnostic algorithm

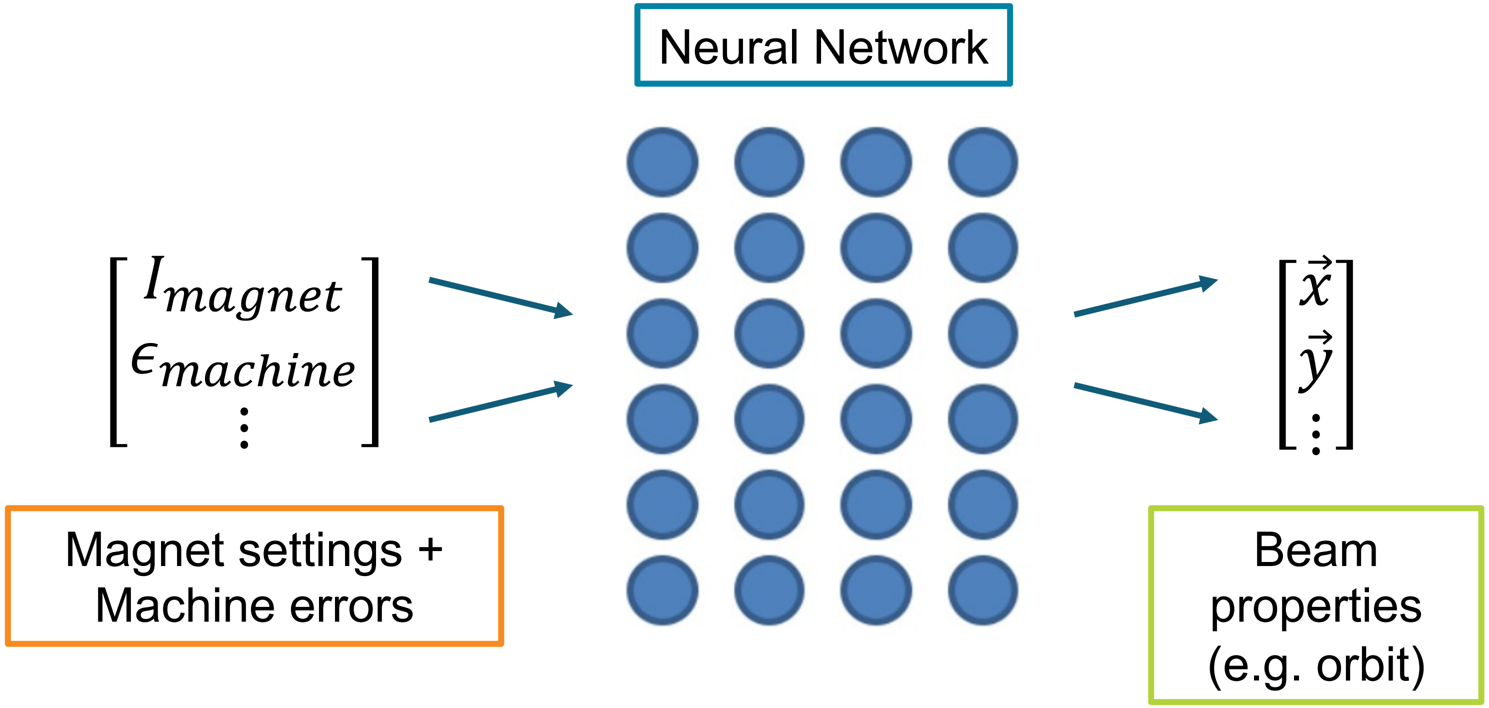

Generalized Gradient Map Tracking in the Siberian Snakes of the Alternating Gradient Synchrotron

Brookhaven National Laboratory

CLASSE
Cornell Laboratory for Accelerator-based ScienceS & Education

Siberian Snake

- Rotates particle spin about an axis in the horizontal plane, without affecting orbit motion, to avoid depolarizing spin resonances

- In the AGS and RHIC: helically twisted dipoles

- Spin tune ν_{sp} of a ring with a Siberian snake of strength s is given by:

$$\cos \pi\nu_{sp} = \cos\frac{s\pi}{2}\cos \pi G\gamma$$

- Full Siberian snake ($s = 1$) rotates spin by $180°$, partial Siberian snake ($s < 1$) is referred to as a percentage of the full snake

Siberian snakes in the AGS

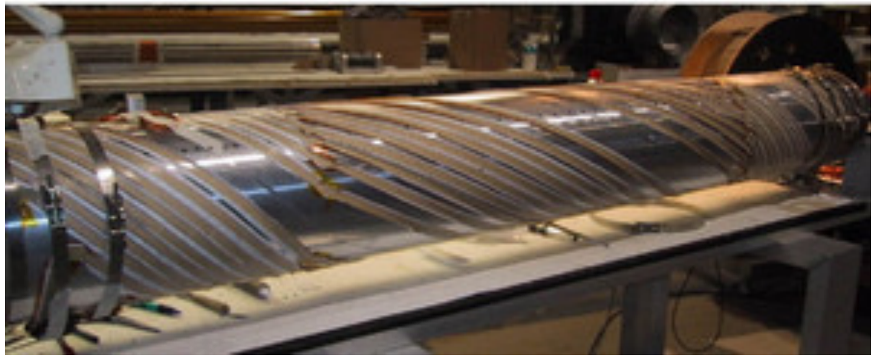

warm (top), cold (bottom)

Siberian Snake in the AGS

- Two partial Siberian snakes 120° apart in the AGS
- Partial snakes cause less orbit disturbances and require shorter straight sections
- 5.9% normal conducting (warm) snake
- Super-conducting (cold) snake capable of up to 22%
- 65% polarization was achieved for acceleration of $1.5{\times}10^{11}$ protons/bunch to 24 GeV in 2007

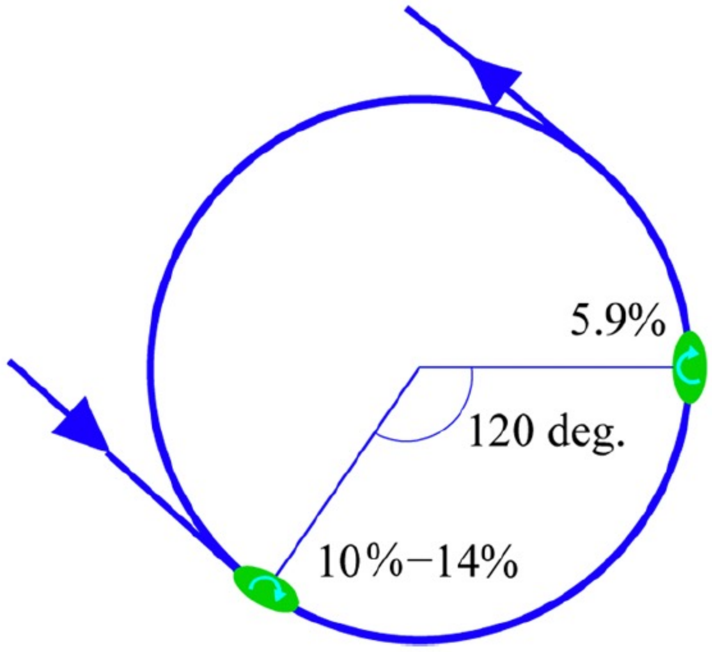

Generalized Gradient (GG)

- In spherical coordinates (ρ, ϕ, z), scalar potential ψ of the magnetic field can be written as:

$$\psi = \sum_{m=0}^{\infty} \psi_{m,c}(\rho, z)\cos(m\phi) + \psi_{m,s}(\rho, z)\sin(m\phi)$$

- The function $\psi_{m,\alpha}$ ($\alpha = c$ or s) can be expressed as a Taylor series in ρ:

$$\psi_{m,\alpha} = \sum_{n=0}^{\infty} \frac{(-1)^{n+1} m!}{4^n n!\,(n+m)!} \rho^{2n+m} C_{m,\alpha}^{[2n]}(z)$$

- $C_{m,\alpha}$ are the generalized gradients, and the superscript $[2n]$ indicates the $2n^{th}$ derivative of $C_{m,\alpha}$

- In practical application, a finite set of $C_{m,\alpha}$ are chosen to represent the field, and the Taylor series for each $C_{m,\alpha}$ is truncated at some order N

- In Bmad, the GG fitting algorithm allows user to pick values of m for $C_{m,\alpha}$ and truncate order N

GG tracking results: magnetic field

- GG maps are generated with $m = 1, 3, 5, 7$ for $C_{m,\alpha}$ (both cos and sin terms), the Taylor series is truncated at order $N = 5$
- Magnetic field values reconstructed from GG fitting algorithm (left) matches the original grid field tables (right)

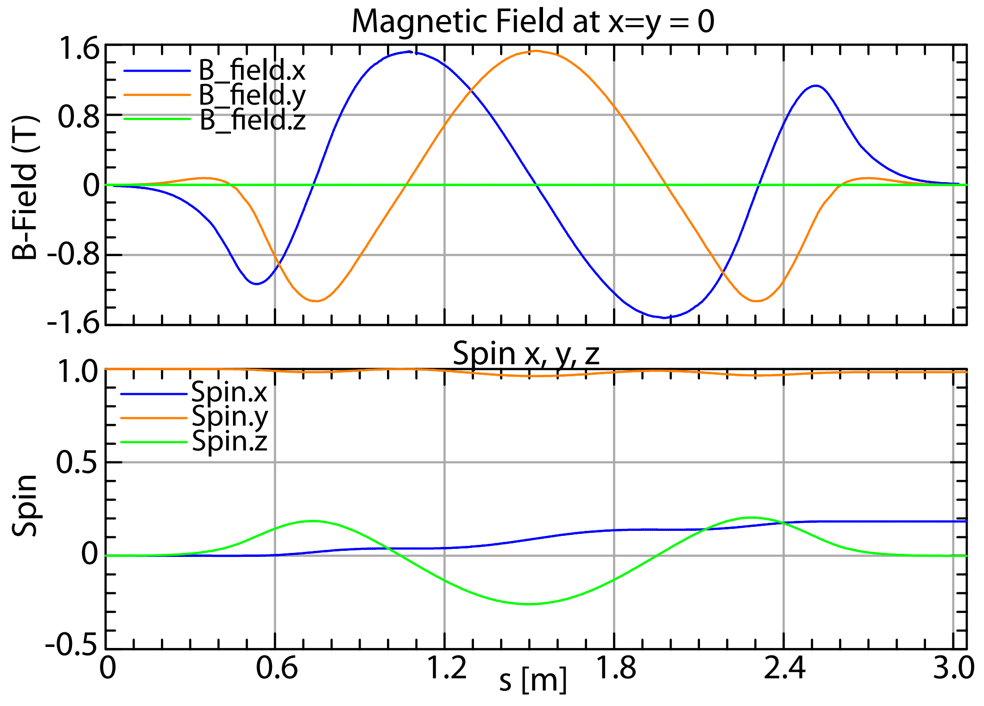

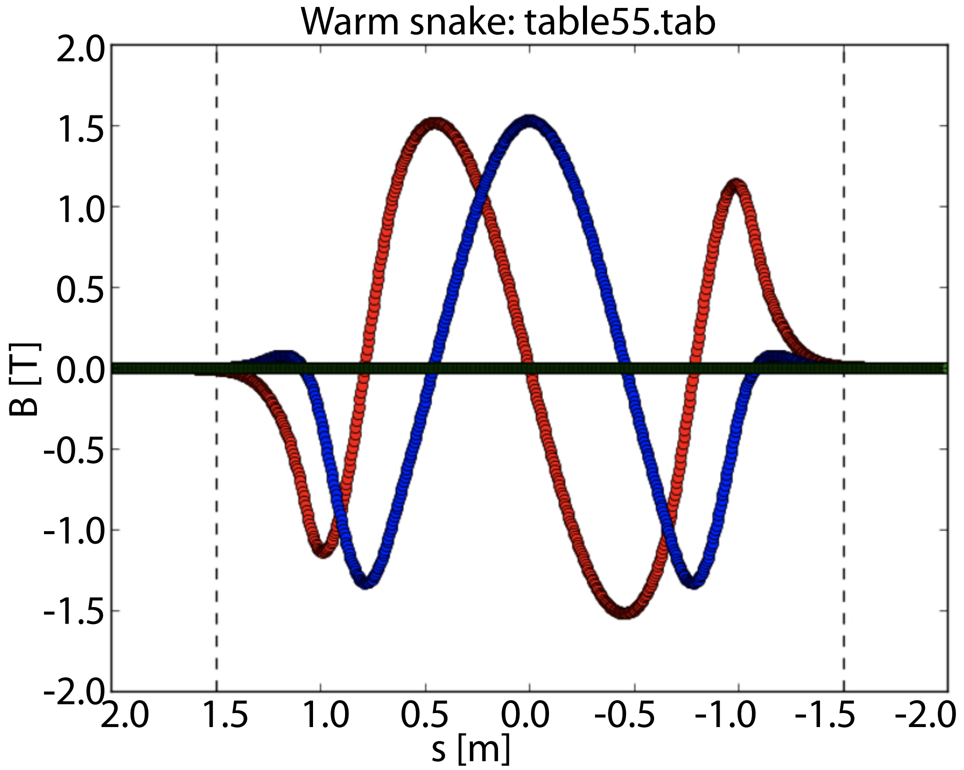

GG tracking results: twiss & orbit

- GG map (left) produces accurate beta function and orbit tracking results compared to grid field table (right)

GG map

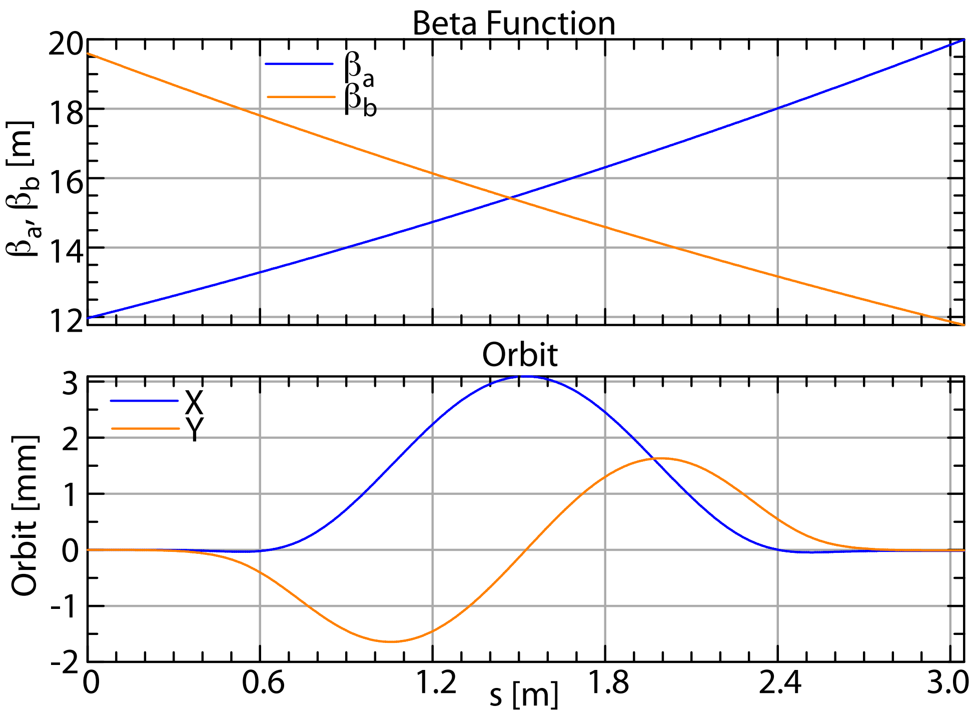

Grid table

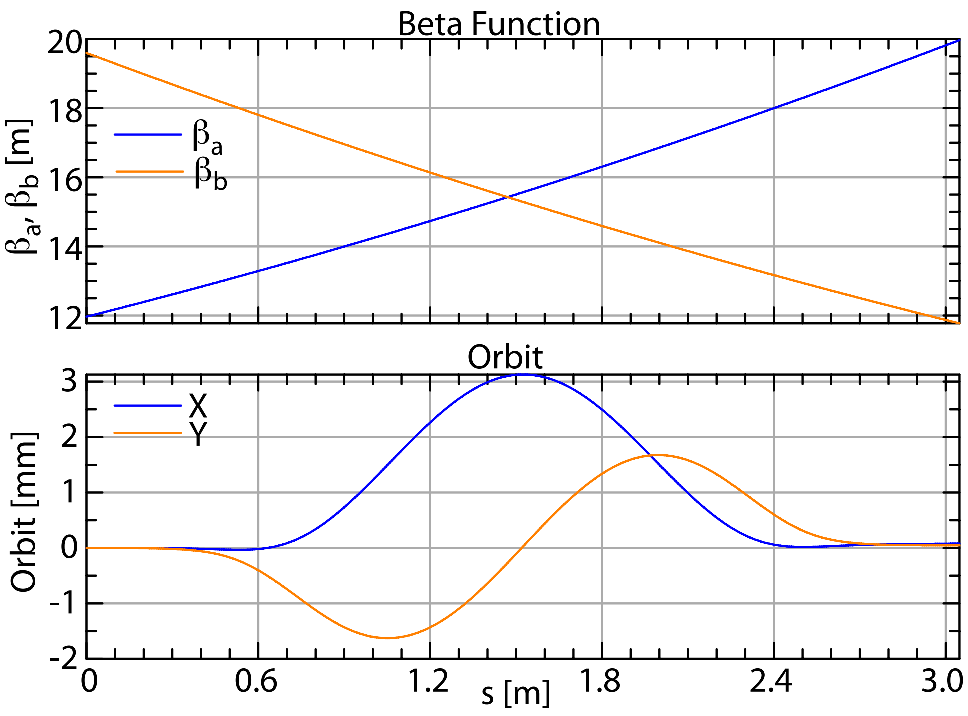

GG tracking results: snake strength

- Track three particles with three initial spin configurations: (1,0,0), (0,1,0), and (0,0,1). The final spin after the snake is rotated by 3-D rotation matrix $\underline{R}$:

$$\underline{R} = \begin{pmatrix} \cos\theta & \sin\theta & 0 \\ -\sin\theta & \cos\theta & 0 \\ 0 & 0 & 1 \end{pmatrix}$$

- Snake strength is then calculated as the ratio $\theta/180°$ in percentage form
- GG map generates accurate snake strengths for both snakes

AGS Snake Strength Calculation Results

Snake	GG map	Grid table
Warm	5.9%	5.86%
Cold	11.4%	11.4%

GG tracking results: tracking time

- Compare three tracking methods:
  - Taylor map tracking derived from GG field map
  - Runge-Kutta tracking using grid table
  - Tracking using matrices generated for specific current and energy settings (traditional way for MAD simulation)
- GG maps are 1000 times faster than grid table, matrix generated at prefixed energy is fastest but has no spin rotation simulation

AGS Snakes Tracking Times (sec)

Snake	GG map	Grid table	Matrix
warm	1.7×10^{-5}	1.63×10^{-2}	2.7×10^{-6}
cold	1.98×10^{-5}	2.42×10^{-2}	3.2×10^{-6}

Current to Magnet Strength Calibration with Neural Network at the AGS Booster

Alternating Gradient Synchrotron (AGS) Booster

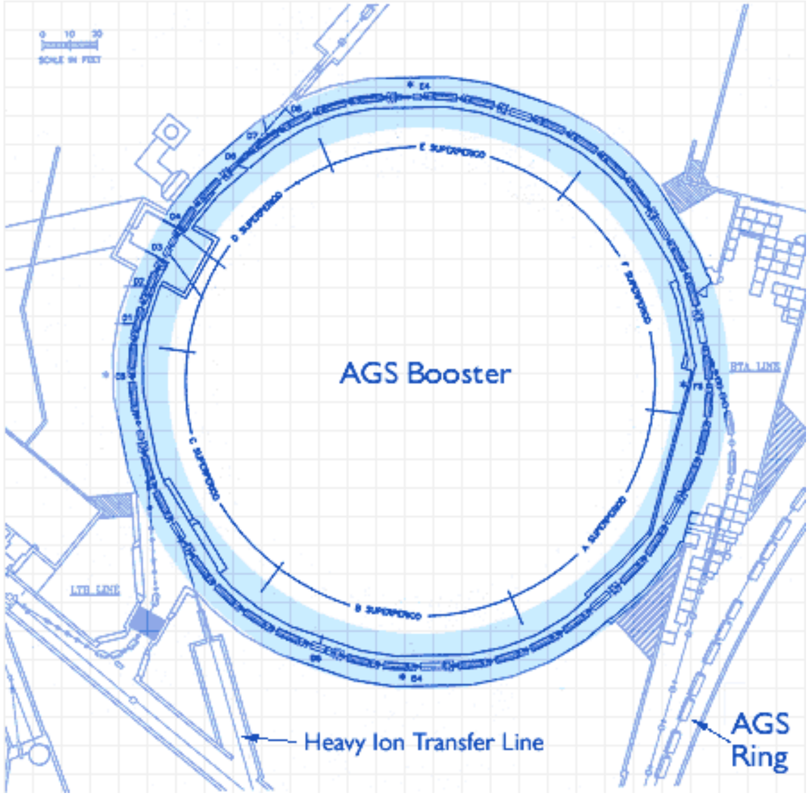

- Pre-accelerate particles entering the AGS ring
- Accepts heavy ions from EBIS or protons from 200 MeV Linac
- Serves as heavy ion source for NASA Space Radiation Laboratory (NSRL)
- 6 super-periods (A to F), 72 main magnets

Magnet current to strength mapping

- **<u>Magnet transfer function</u>**: mapping between the power supply (PS) current and the resulting strength of a magnet

- Example: 5^{th} order polynomial for Booster quadrupoles

- Transfer functions are measured before the magnets were installed in the ring, and there is <u>no existing way to verify them</u> after installation.

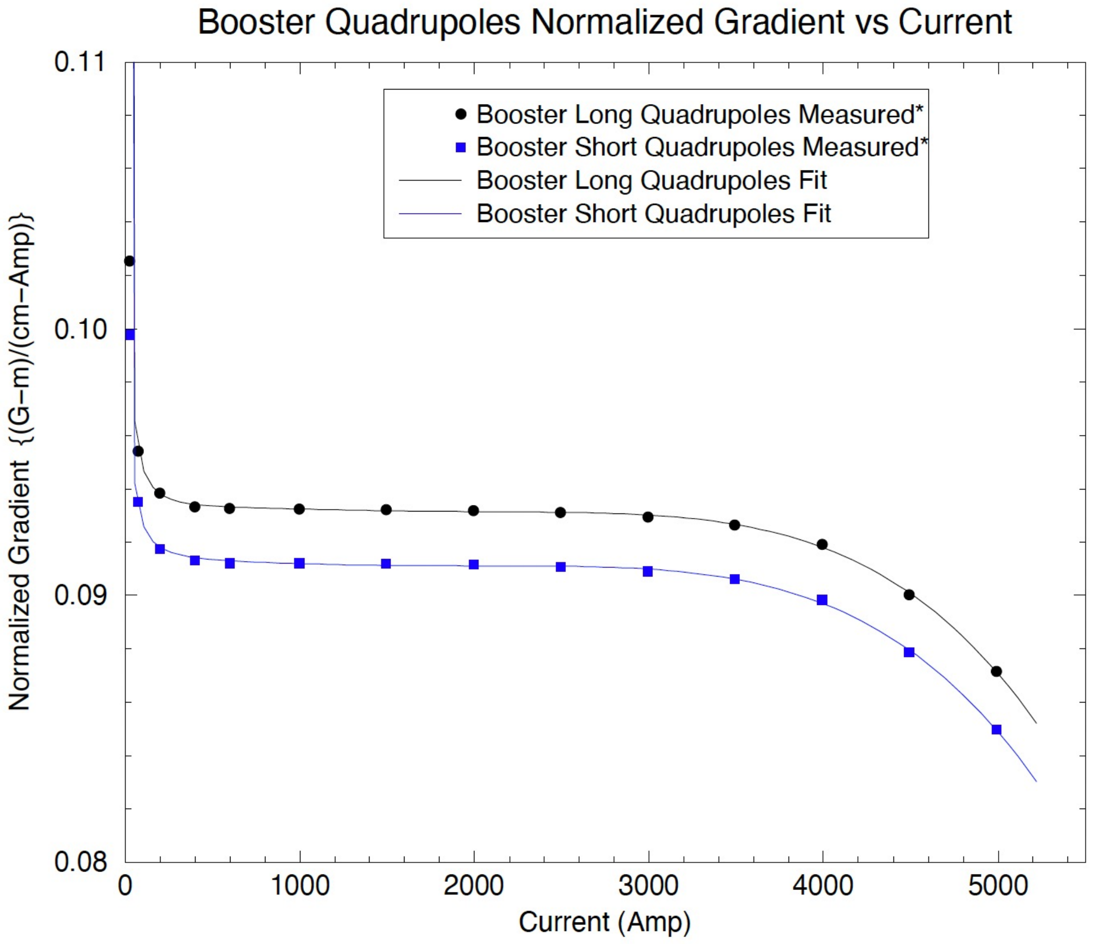

Calibration workflow

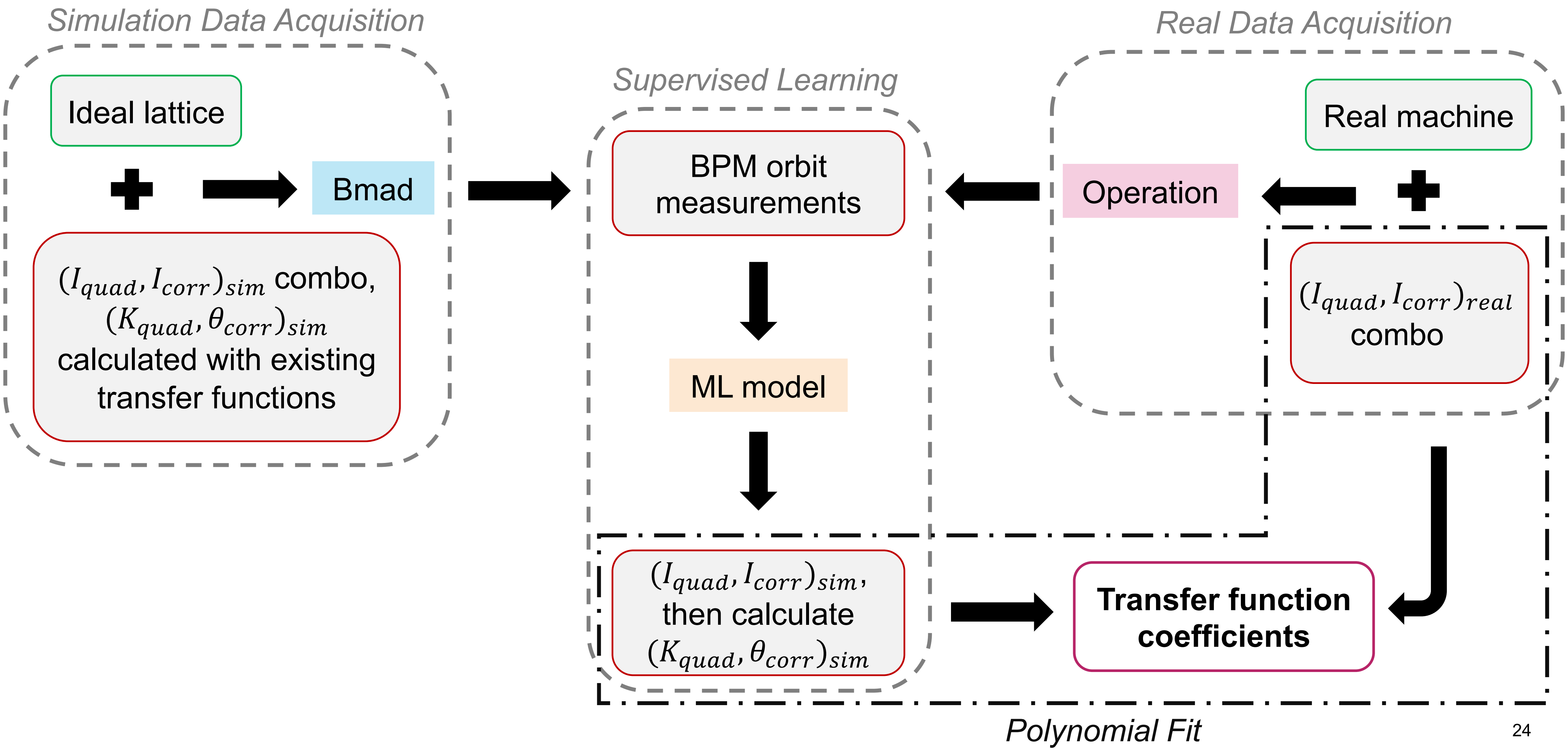

Preliminary training result in one plane

- Input y orbit under different quadrupole PS currents → Output corresponding vertical quadrupole strength
- Initial data was collected with magnet settings within the linear range of the transfer function, working on collecting more data
- Trained on 800 data pairs, tested on 200 data pairs: accuracy = 99.5%

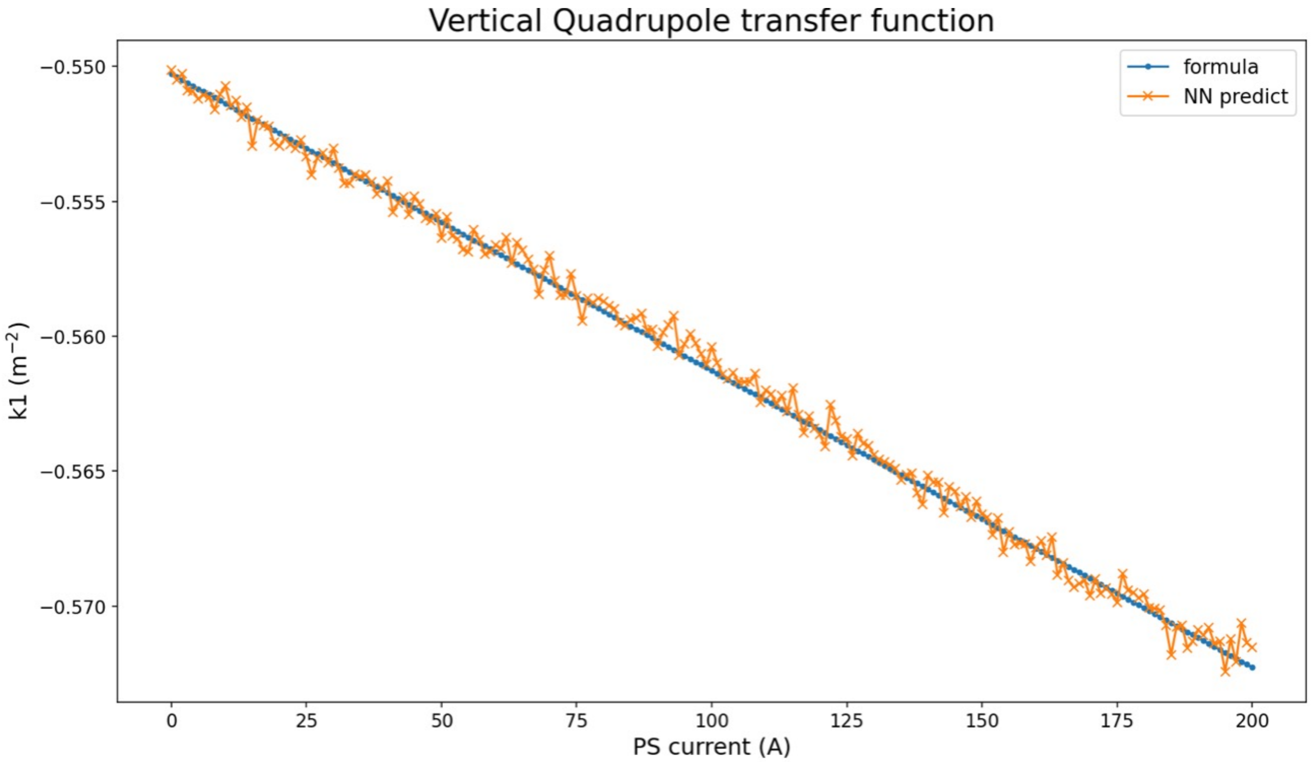

CAD script to get real orbit responses

- Script development with Collider Accelerator Department (CAD) Controls Group
- FunctionEditor: send trapezoid-like time-dependent function to corrector power supplies
- Script sets three corrector settings: positive, zero, negative; and save corresponding orbits

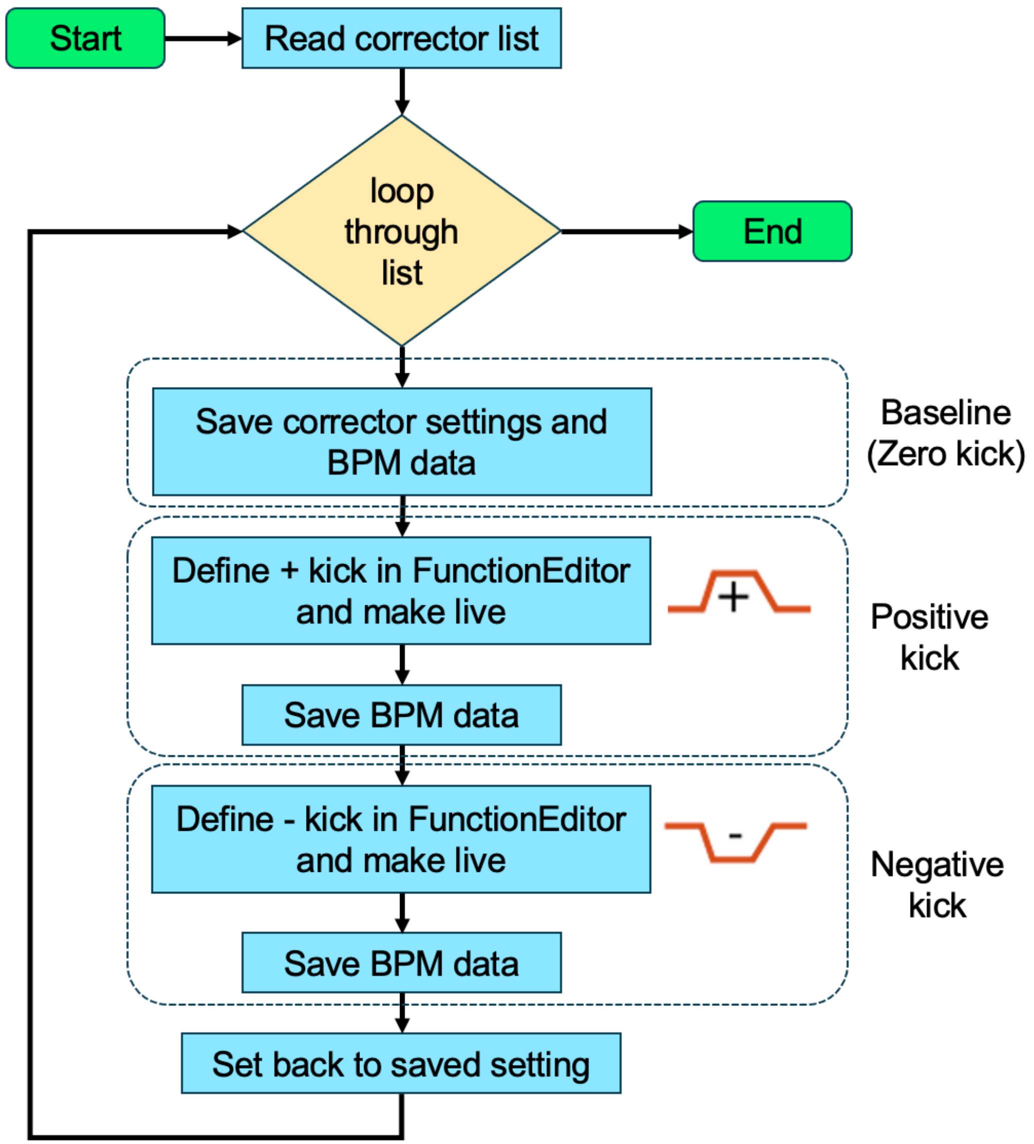

Booster magnet misalignment

- Magnet location in real machine from 2015 survey data
- Misalignment data for quadrupoles and dipoles

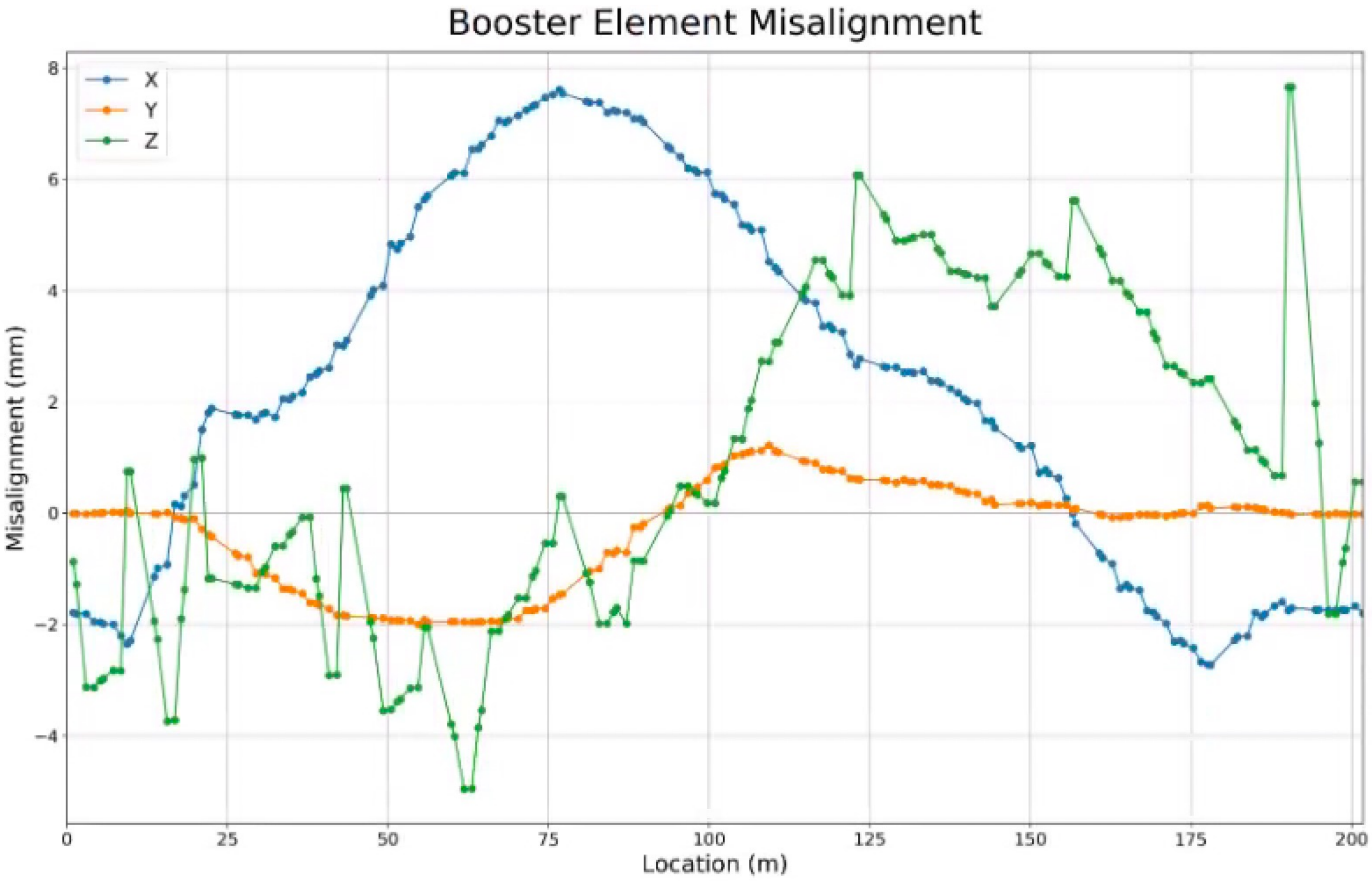

Booster orbit response mapping

$$\left(I_{quad}, I_{corr}, \phi\right) \Leftrightarrow \left(X_{BPM}^{\left(I_{quad}^{(1)}, I_{corr}^{(1)}, \phi^{(1)}\right)}, X_{BPM}^{\left(I_{quad}^{(2)}, I_{corr}^{(2)}, \phi^{(2)}\right)}, \dots\right)$$

- Control: power supply currents of quadrupoles and correctors
- Parameter ϕ: other parameters that affect the orbit but not in our control (e.g., main magnet current, magnet misalignment…)
- Output: orbit at the BPMs with certain current configuration
- To Do:
  - determine what goes in ϕ (e.g., magnet misalignment), and their range of values + errors
  - determine if controls have error distribution (setpoint vs measured)

Neural network for orbit response mapping

$$\left(I_{quad}, I_{corr}, \phi\right) \overset{NN}{\Longleftarrow\!=\!=\!\Longrightarrow} \left(X_{BPM}^{(I_{quad}^{(1)}, I_{corr}^{(1)})}, X_{BPM}^{(I_{quad}^{(2)}, I_{corr}^{(2)})}, \dots\right)$$

- Neural network is better long-term (and on bigger machine) due to faster speed
- Parameters ϕ can be inferenced from real orbit data
- Need to figure out a good sampling method due to tune resonance constraints on I_{quad}
- Working with applied math experts on how to best handle model building and inferences

Bmad vs. Madx: offset definitions

- Rotation around y axis: x_pitch = dtheta, around x axis: y_pitch = - dphi
- Note: x_pitch and y_pitch rotations are about the center of the element, dtheta and dphi misalignments rotate around the entrance point
- Rotation around z axis: tilt = dpsi or tilt

Bmad

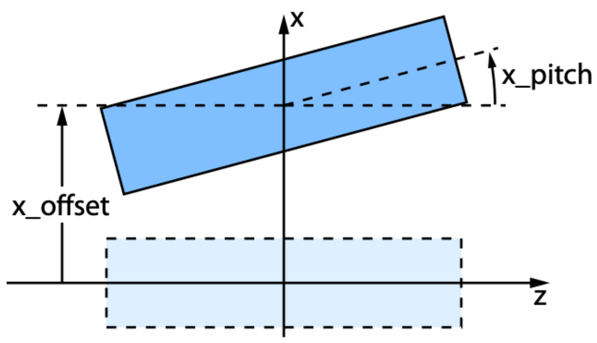

Figure 5.1: Geometry of Pitch and Offset attributes

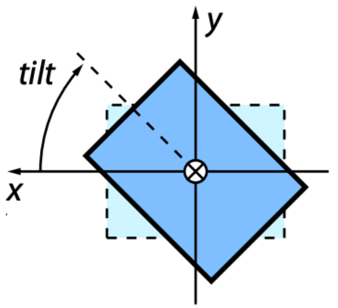

Figure 5.2: Geometry of a Tilt

MAD-X

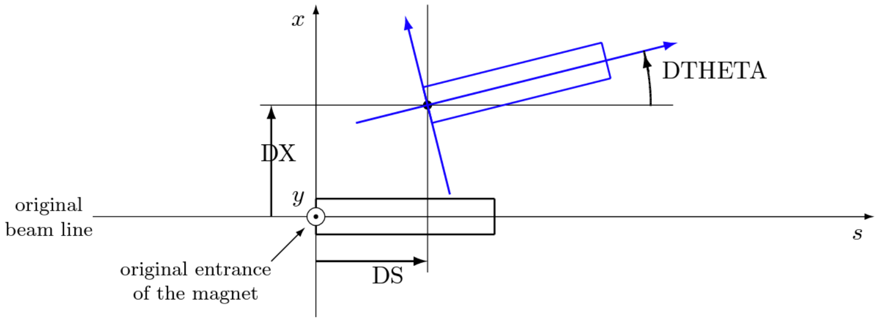

Figure 24.1: Alignment errors in the (x, s)-plane

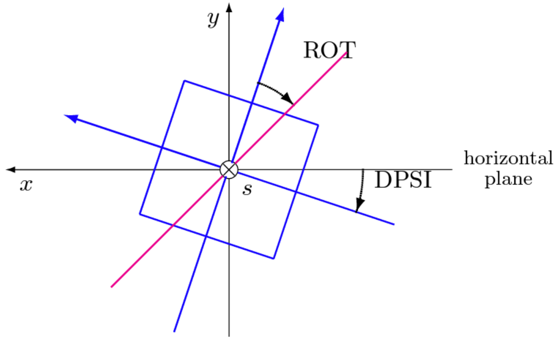

Figure 24.2: Alignment errors in the (x, y)-plane

Quad offset: QVD1

Location	S (m)	dX (mm)	dY (mm)	dZ (mm)
upstream	0.989875	-1.7853929	-0.0085697	-1.7853929
downstream	1.493875	-1.8057309	-0.0074198	-1.2771865

- Bmad misalign w.r.t. element center, Madx misalign w.r.t. element start
- Bmad offsets → average offsets
- Madx offsets → upstream offsets

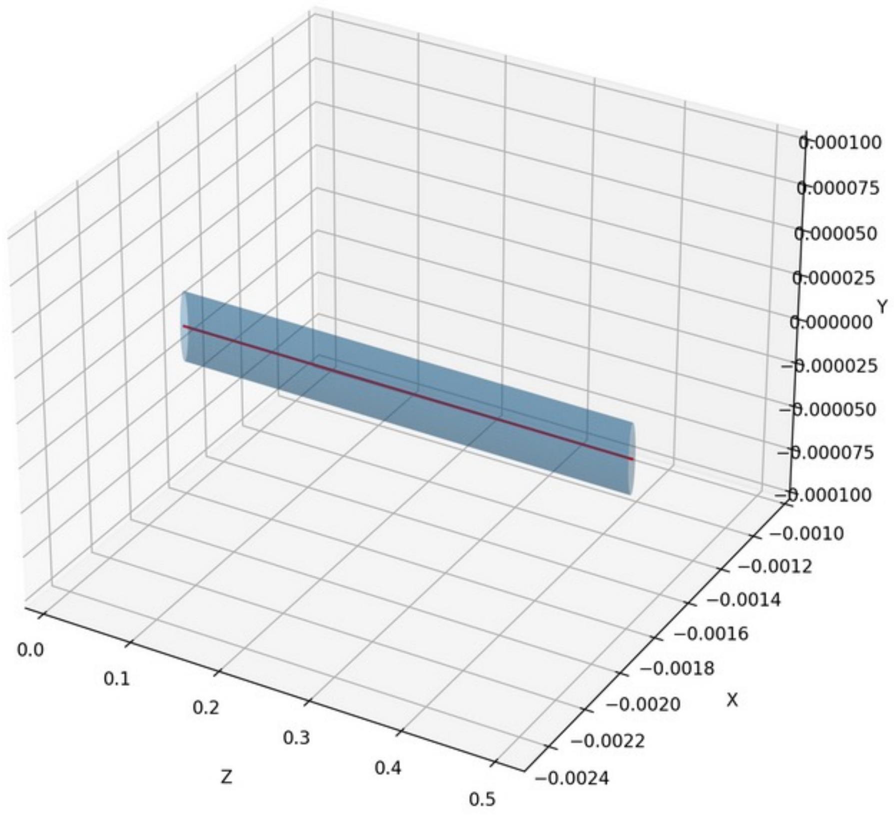

x_pitch = -4.045e-5 rad
y_pitch = -2.28e-6 rad
tilt = 4.039e-5 rad

dtheta = -4.045e-5 rad
dphi = 2.28e-6 rad
dpsi/tilt = 4.039e-5 rad

Add misalignment to all magnets

- Bmad misalign w.r.t. element center, Madx misalign w.r.t. element start
- Bmad offsets → average offsets, Madx offsets → upstream offsets
- Tracking results agree after adding offsets and rotations

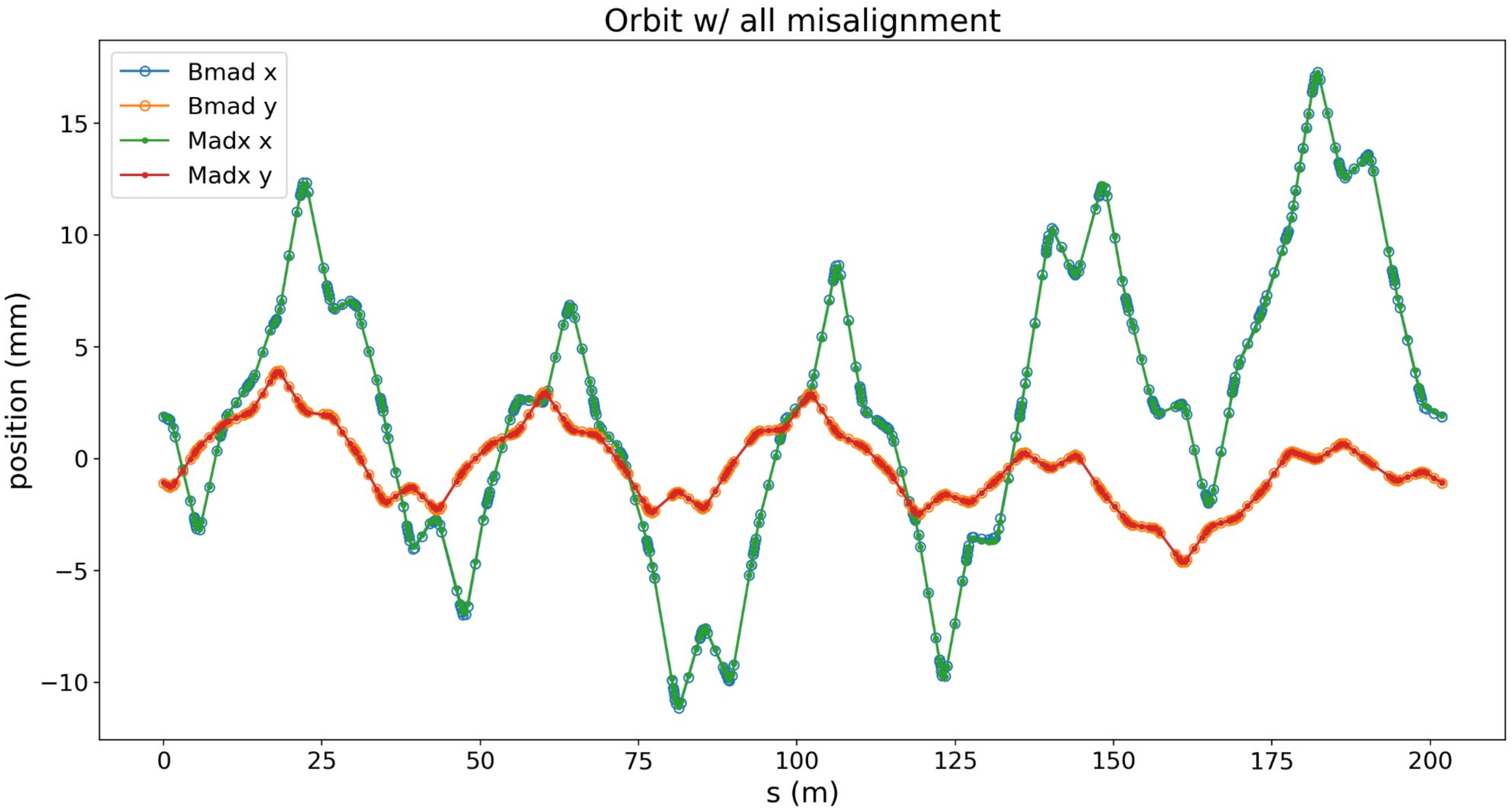

Sample data in tune space

- Sample non-zero H & V quadrupole settings that don't hit a resonance
- Quadrupole PS current range 0 – 400 A
- Produce double-plane orbit response without hitting resonance

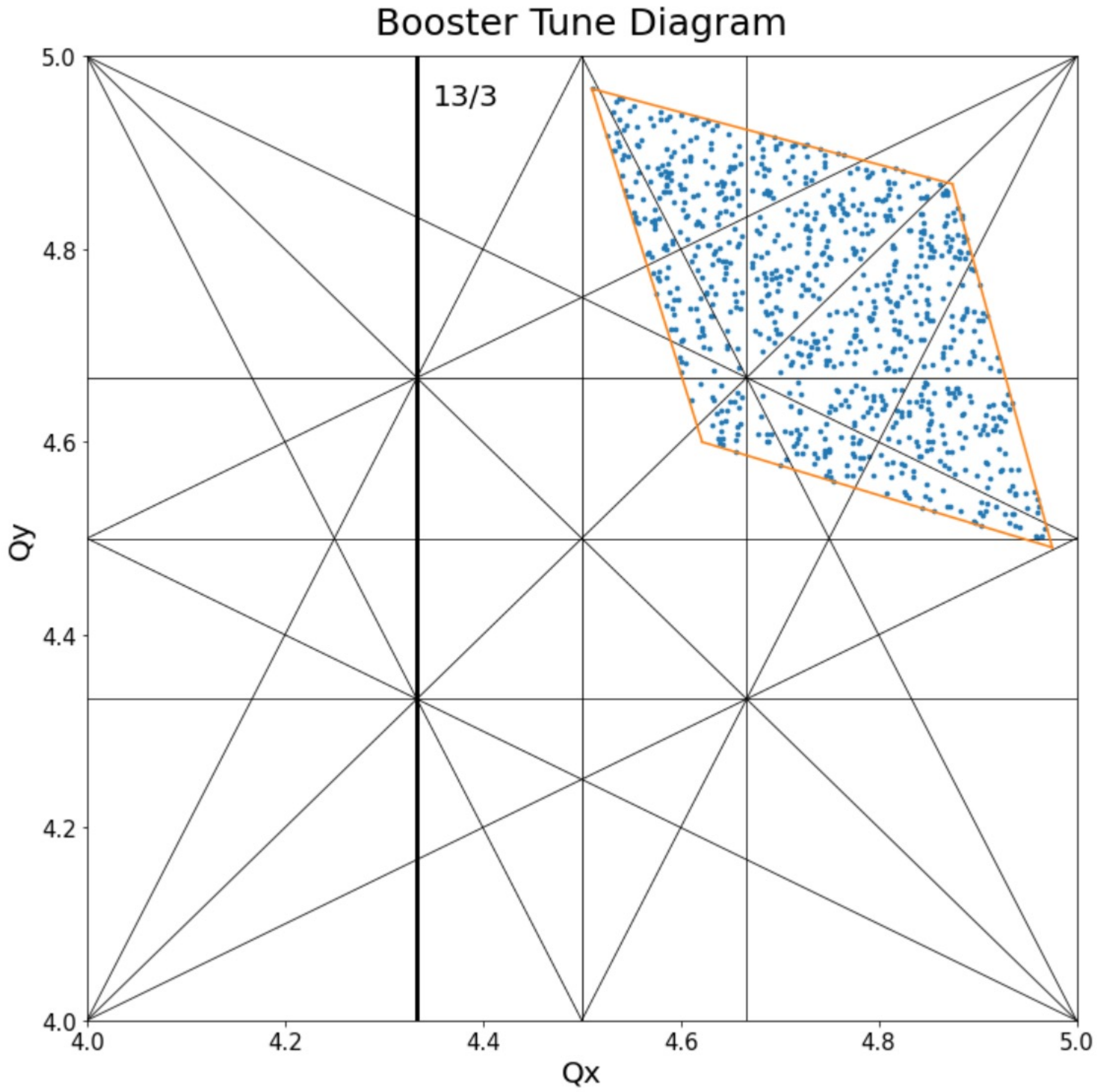

Preliminary training result in both planes

- The ends are less accurate in both planes
- Preliminary results, need more exploration on best model structure

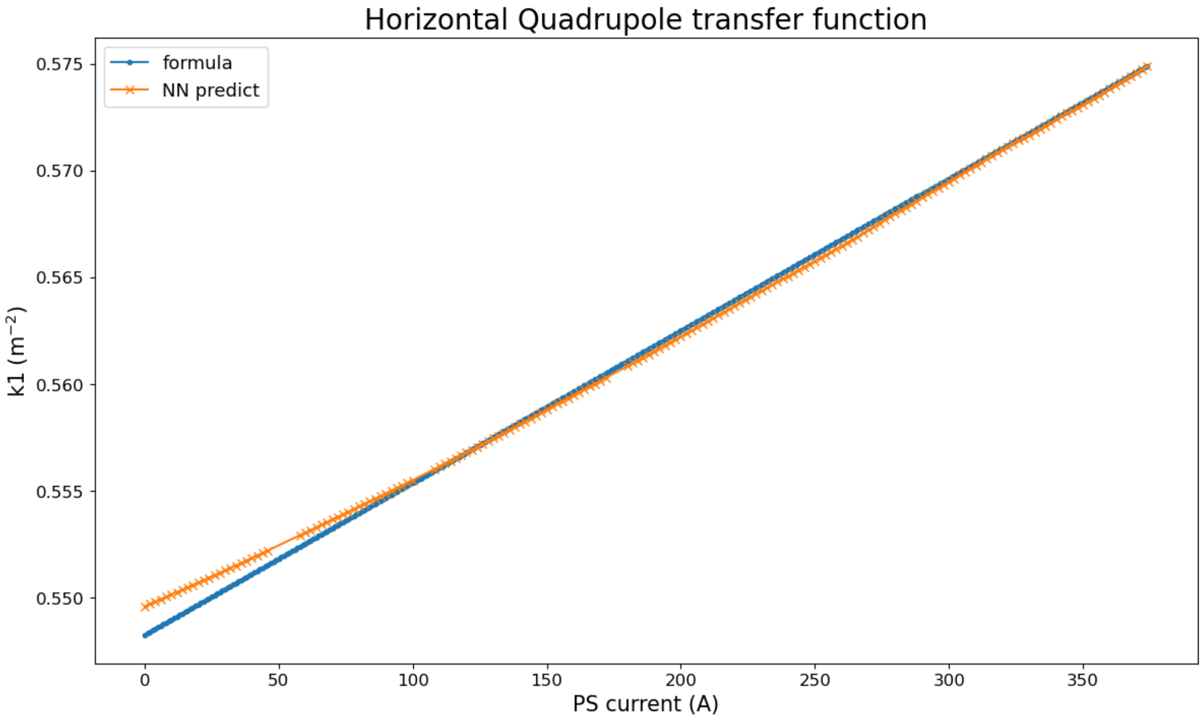

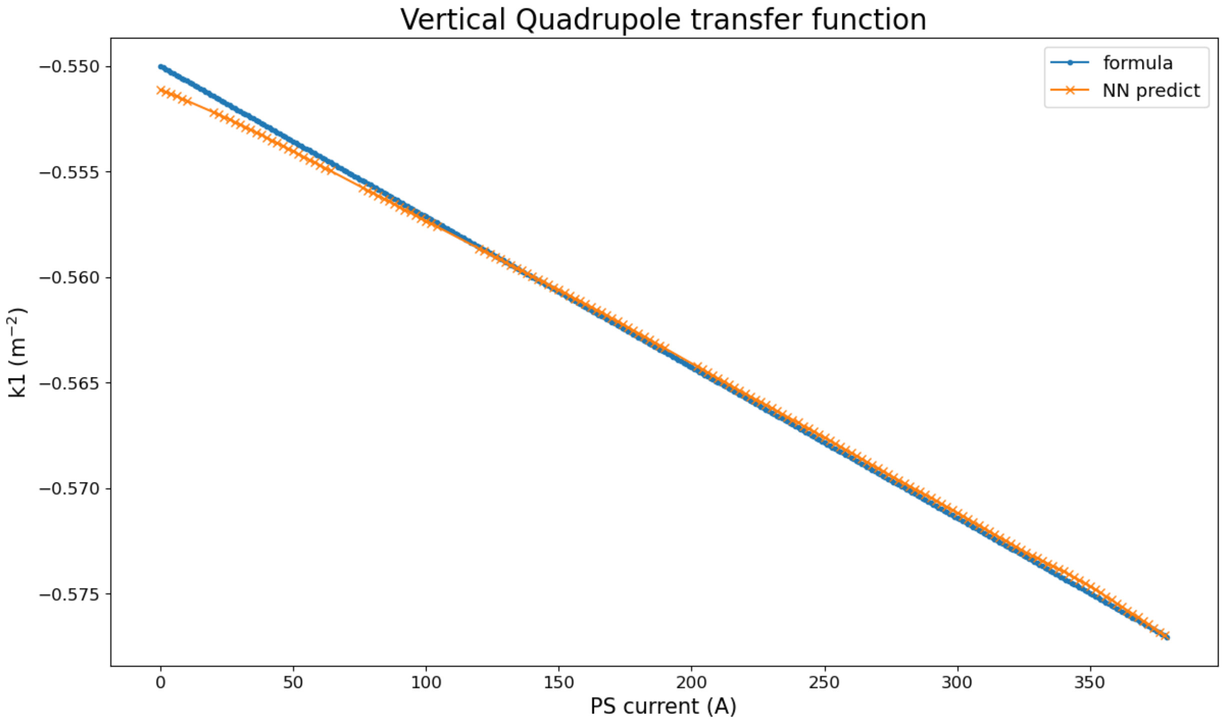

Future work: Optimization with ML

Control parameters + Environmental factors

Neural Network

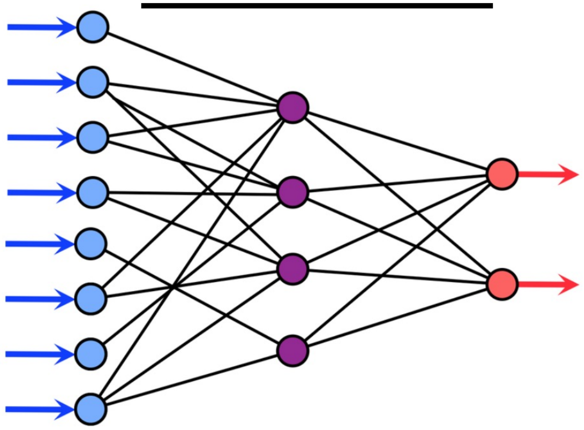

Evaluation Metric (e.g., agreement with real measurements)

Bayesian Optimization

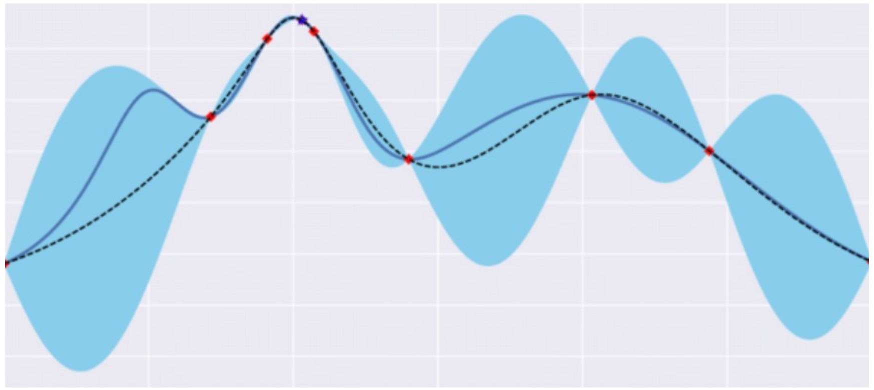

Find best settings for desired machine state

Thanks

Brookhaven National Laboratory

- Petra Adams, Kevin Brown, Bhawin Dhital, Yuan Gao, Levente Hajdu, Kiel Hock, John Morris, Seth Nemesure, Vincent Schoefer

CLASSE
Cornell Laboratory for Accelerator-based ScienceS & Education

- Eiad Hamwi, Georg Hoffstaetter de Torquat, David Sagan

Stony Brook University

- Weining Dai, Bohong Huang, Thomas Robertazzi

References

- [1] W. Lin, D. Sagan, G.H. Hoffstaetter, B. Huang, W. Dai, T. Robertazzi, V. Schoefer, K.A. Brown, "Machine Learning Applications for Orbit and Optics Correction at the Alternating Gradient Synchrotron", in *Proc. IPAC'23*, Venice, Italy, May 2023.

- [2] W. Lin, E. Hamwi, D. Sagan, G.H. Hoffstaetter, "Generalized Gradient Map Tracking in the Siberian Snakes of the AGS and RHIC", in *Proc. IPAC'23*, Venice, Italy, May 2023.

- [3] W. Lin, D. Sagan, G.H. Hoffstaetter, B. Huang, W. Dai, T. Robertazzi, V. Schoefer, P. Adams, B. Dhital, Y. Gao, K.A. Brown, "AGS Booster Beam-based Main Quadrupole Transfer Function Measurements", in *Proc. IPAC'23*, Venice, Italy, May 2023.